The impact of optical comb stability on waveforms generated via spectral line-by-line pulse shaping

Chen-Bin Huang, Zhi Jiang, Daniel E. Leaird, Andrew M. Weiner

School of Electrical and Computer Engineering, Purdue University
465 Northwestern Avenue, West Lafayette, IN 47907-2035
robinh@purdue.edu, zjiang@purdue.edu, leaird@purdue.edu, amw@ecn.purdue.edu

Abstract: Optical arbitrary waveform generation using the line-by-line pulse shaping technique has been shown to be sensitive to variations in the offset frequency of the input frequency comb due to time-domain waveform interference. Here we present a frequency-domain model that is able to predict waveform changes arising from offset frequency variations. In experiments we controllably shift the frequency of a comb derived from a phase-modulated CW laser, which allows us to quantitatively investigate waveforms generated by pulse shaping as a function of offset frequency. Experimental data are in excellent agreement with the predictions of our frequency-domain model. In addition, we propose and analyze new waveforms designed for monitoring of offset frequency variations by pulse shaping.

OCIS codes: (320.5540) Pulse shaping, (070.4790) Optical spectrum analysis, (120.3930) Metrological instrumentation, (230.2090) Electro-optical devices, (140.4050) Mode-locked lasers.

References and links

1. S. T. Cundiff, J. Ye, and J. L. Hall, "Optical frequency synthesis based on mode-locked lasers," Rev. Sci. Inst. **72**, 3749-3771 (2001).
2. A. M. Weiner, "Femtosecond pulse shaping using spatial light modulators," Rev. Sci. Inst. **71**, 1929-1960 (2000).
3. Z. Jiang, D. E. Leaird, and A. M. Weiner, "Line-by-line shaping control for optical arbitrary waveform generation," Opt. Express **13**, 10431-10439 (2005).
4. Z. Jiang, D. S. Seo, D. E. Leaird, and A. M. Weiner, "Spectral line-by-line pulse shaping," Opt. Lett. **30**, 1557-1559 (2005).
5. S. Hisatake, Y. Nakase, K. Shibuya, and T. Kobayashi, "Generation of flat power-envelope terahertz-wide modulation sidebands from a continuous-wave laser based on an external electro-optic phase modulator," Opt. Lett. **30**, 777-779 (2005).
6. Z. Jiang, D. E. Leaird, and A. M. Weiner, "Optical processing based on spectral line-by-line pulse shaping on a phase modulated CW laser," IEEE J. Quantum Electron. **42**, 657-665 (2006).
7. Z. Jiang, D. E. Leaird, and A. M. Weiner, "Optical arbitrary waveform generation and characterization using spectral line-by-line control," IEEE J. Lightwave Technol. **24**, 2487-2494 (2006).
8. T. Kobayashi, H. Yao, K. Amano, Y. Fukushima, A. Morimoto, and T. Sueta, "Optical pulse compression using high-frequency electrooptic phase modulation," IEEE J. Quantum Electron. **24**, 382-387 (1988).

1. Introduction and problem description

Optical combs are comprised of spectral lines that are evenly spaced and determined by the source repetition frequency and with well defined phase relations between the lines [1]. Optical pulse shaping techniques, in which phase and amplitude manipulation of optical spectral components allow synthesis of user-specified ultrashort pulse fields according to a Fourier-Transform relationship, have been developed and widely adopted [2]. Previous pulse shapers, however, have generally manipulated groups of spectral lines rather than individual

#76023 - $15.00 USD Received 13 October 2006; accepted 10 December 2006

lines due to difficulty in building a pulse shaper capable of resolving each spectral line at typical repetition frequencies (≤1 GHz) for practical optical combs generated by mode-locked lasers. This result in waveform bursts that are separated in time with low duty factor and that are insensitive to the variation of the frequency offset of the comb lines. However, the phase and amplitude of each individual comb line should be independently controlled in order to approach true optical arbitrary waveform generation (O-AWG) [3]. A pulse shaper capable of implementing line-by-line control can generate shaped waveforms spanning the full time period (T) between the initial mode-locked pulses (100% duty factor). From a time-domain perspective, in the line-by-line regime waveform contributions arising from adjacent pulses in the mode-locked train overlap and interfere. The effect of the interference depends on the relative phase between adjacent mode-locked pulses, which is proportional to the comb offset frequency. Consequently, frequency fluctuations of the mode-locked comb translate into time-dependent waveform noise in line-by-line pulse shaping. This effect fundamentally links the field of pulse shaping with the field of frequency-stabilized mode-locked lasers (combs).

The first observation of such waveform noise in line-by-line pulse shaping was reported in Ref. [4] by selecting two comb lines from a harmonically mode-locked fiber laser without active frequency stabilization. The laser was operated at ~10 GHz repetition rate, which made it possible to resolve individual lines using a carefully designed pulse shaper. Selecting only two spectral lines from the broader input spectrum yields a cosine waveform in the time-domain. The relative delay of the peaks of the cosine can be tuned by using the pulse shaper to control the phase (Φ) of one of the selected lines. The pulses are shifted by T/2 (half of the pulse period) if $\Phi=\pi$ is applied to a single line. The experiments in Ref. [4] showed that waveform noise related to optical frequency fluctuations was much larger for the $\Phi=\pi$ case than for the $\Phi=0$ case. This difference was understood by observing that largest waveform noise is expected at temporal positions where adjacent input pulses provide equal contributions and hence largest interference, which occurs exactly between the original pulses (at T/2). This time-domain picture provides a successful qualitative explanation of the experimental observations.

In this paper, we present the first quantitative investigation of the impact of optical comb frequency offsets on the time-domain intensity waveforms generated via spectral line-by-line pulse shaping. Instead of a harmonically mode-locked laser, we employ an optical comb generated by a phase-modulated CW (PMCW) laser. By shifting the center wavelength of the CW laser, the wavelength of the entire comb can be shifted accordingly, while leaving the relative powers, spacing and phases of the lines unchanged. PMCW combs are simple in configuration, stable even at the high repetition rates of interest here, and provide much more flexible tuning over repetition rate and comb offset frequency compared to harmonically mode-locked lasers. Broad PMCW combs have seen significant recent progress [5]. Further, line-by-line shaping on a PMCW comb has been reported previously [6], demonstrating the comb stability necessary for optical waveform processing. Together these attributes of the PMCW laser enable quantitative study of the linkage between variations in comb frequency and pulse shaper output.

Figure 1(a) shows the schematic experimental setup. A tunable CW laser is phase-modulated using a lithium niobate phase modulator (12.5 GHz bandwidth, V_π ~5V at 10 GHz) driven at f_{rep}=9 GHz (~1.6 V_π peak to peak) to obtain an optical comb with lines spaced by 9 GHz as shown in Fig. 1(b). The frequencies are defined relative to the CW laser frequency. The comb spectrum is observed using an optical spectrum analyzer (OSA) with 0.01 nm resolution. Lines at frequencies higher than the CW laser are all in phase as measured using the method reported in Ref. [7]. An expanded view of a few lines is shown in the inset on a linear scale and normalized to line {1}. Using the pulse shaper to select the two lines marked {1, 2} and detuning the center wavelength of the CW laser while the modulation frequency f_{rep} is fixed, we are able to emulate the effects of the frequency offsets in the mode-locked laser of [4].

#76023 - $15.00 USD Received 13 October 2006; accepted 10 December 2006

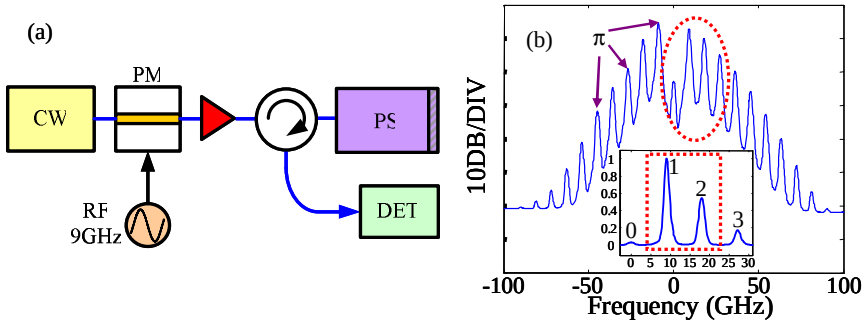

Fig. 1. (a). Schematic of experimental setup. PM: phase modulator; PS: reflective line-by-line pulse shaper; DET: to OSA or sampling scope. (b). Optical spectrum of the phase-modulated CW laser frequency scale relative to the CW line. The frequency lines are separated by 9GHz. Inset: lines circled are expanded and plotted on a linear scale. Lines {1, 2} are selected by the line-by-line shaper.

Figure 2 shows experimental results where only two lines, {1, 2}, are transmitted through the line-by-line shaper. Figures 2(a) and 2(c) show the spectra obtained by detuning the PMCW comb with frequency offset values of {0, 7, 14, 21, 28, 35, 42, and 49}% with either $\Phi=0$ or $\Phi=\pi$ applied to line {1}, respectively. The arrows in Fig. 2 indicate the initial line positions (zero offset) and the direction of detuning as the frequency offset is applied. Figures 2(b) and 2(d) show time-domain intensity waveforms corresponding to the frequency offsets. Intensity waveforms are obtained by sending shaped spectral lines to a 60 GHz photo-detector whose output is measured by a sampling scope with 50 GHz bandwidth. The vertical arrows indicate the evolution of the intensity as the optical frequency offset increases. Throughout this paper, intensity waveforms are normalized to the peak value measured with zero frequency offset. The temporal delay of intensity waveforms comprised of two frequency lines as a function of the relative phase setting is related through:

$$\tau(\Phi) = \frac{\Phi}{2\pi} \mathrm{T} \tag{1}$$

where $T=1/f_{rep}$ is the waveform periodicity and Φ is the phase applied to one line. $\tau(\Phi)$ due to the phase settings ($\Phi=0,\pi$) are shown with dashed lines

With the same value of optical frequency offset, peak intensities of the waveforms of Fig. 2(d) ($\Phi=\pi$) change much more strongly with optical frequency variations than those of Fig. 2(c) ($\Phi=0$). This finding is consistent with the results obtained in Ref. [4] using a non-stabilized harmonically mode-locked laser. The implication is that the phase control in pulse shaping is the primary reason for this difference. In addition, dramatic changes in waveform shape are observed in the $\Phi=\pi$ case which do not occur for $\Phi=0$. In this paper we will develop a frequency-domain model that allows quantitative prediction of the results of the experiments shown in Fig. 2, as well as a series of related experiments.

It is worth noting that relatively large offsets are intentionally introduced in this paper, so that the impact of frequency instability on time-domain waveform generation can easily be observed with a sampling scope. However, similar time-domain noise effects are expected to be observable even for smaller frequency fluctuations (offsets), provided that more sensitive diagnostic tools are available.

#76023 - $15.00 USD Received 13 October 2006; accepted 10 December 2006

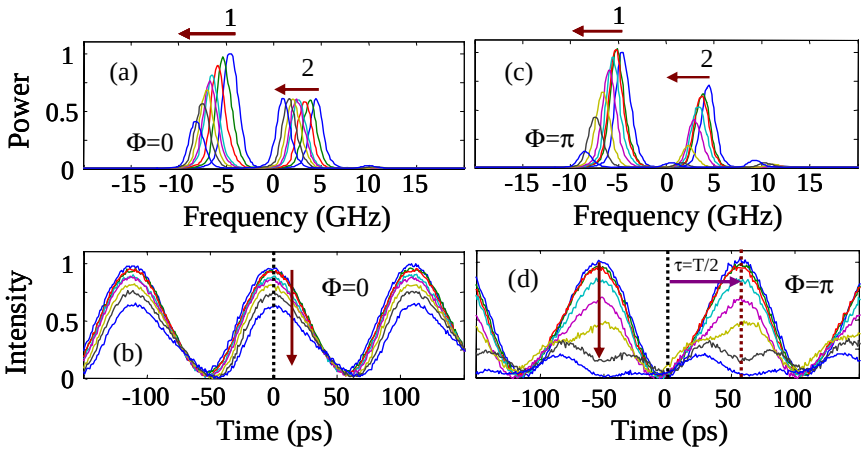

Fig. 2. Experimental results by detuning the PMCW comb with relative frequency offsets of {0, 7, 14, 21, 28, 35, 42 and 49}%. (a, c) Spectra (linear scale in relative frequency) for Φ=0 and Φ=π, respectively. The horizontal arrows indicate the initial line positions and the direction of detuning. (b, d) Time-domain intensities for corresponding frequency offsets for Φ=0 and Φ=π, respectively. The vertical arrows indicate intensity peak variations as the optical frequency offset increases. Zero delay positions are marked by dashed lines. (Video file of 0.96 Mb for Φ=0 and 0.98 Mb for Φ=π.)

The rest of this paper is organized as follows. In section 2, a rigorous frequency-domain model is presented and numerical fit to experimental data is provided. Moreover, correlations between time and frequency-domain pictures are justified experimentally. In section 3, time-domain waveforms that show enhanced sensitivity for monitoring of frequency offset fluctuations are designed and experimentally demonstrated.

2. Modeling and fitting

In the examples shown in Fig. 2, it is apparent that the observed time-domain waveform variations are linked to phase manipulation in the pulse shaping process. We now present a model which explains these observations in the frequency-domain.

2.1 Modeling

For a grating based free-space pulse shaper, the effective frequency-domain filter function H(ω) that characterizes its response as a linear filter can be obtained by convolving the programmable spatial masking function M(x) defined by the liquid crystal modulator (LCM) with the Gaussian intensity profile of a single optical frequency beam:

$$H(\omega) = \left(\frac{2}{\pi w_0^2}\right)^{1/2} \int M(x) e^{\frac{-2(x-\alpha\omega)^2}{w_0^2}} dx \qquad (2)$$

where w_0 is the Gaussian beam radius (half-width at $1/e^2$ of intensity) and α is the spatial dispersion with units cm $(rad/s)^{-1}$ [2]. In the experiment the frequency lines have a 9 GHz spacing, with each line having a Gaussian spatial profile of radius w_0=75 μm. Each LCM pixel has a 100 μm width and a corresponding frequency span of 4.5 GHz; therefore frequency lines are centered on every second LCM pixel. Our line-by-line shaper has α=3.54e-13 cm $(rad/s)^{-1}$ and a full-width at half maximum spectral resolution of 5.31GHz. The spectral resolution is limited here by the width of turning on one single LCM pixel. This obtained resolution ensures observation of temporal overlapping contributions from adjacent pulses. The output fields of the linear filter $E_{out}(\omega)$ is the product of the input field $E_{in}(\omega)$ and the filter function H(ω):

#76023 - $15.00 USD Received 13 October 2006; accepted 10 December 2006

$$E_{out}(\omega) = E_{in}(\omega)H(\omega) \tag{3}$$

Finally, the time-domain envelope function $e_{out}(t)$ is obtained by Fourier transforming the output field:

$$e_{out}(t) = \frac{1}{2\pi}\int E_{out}(\omega)e^{j\omega t}d\omega \tag{4}$$

In Fig. 3(a), a schematic representation of the optical comb lines in absolute position (black solid) and with an initial frequency offset ε_0 (blue dash) are both depicted as arrows. The comb line positions can be described as [1]:

$$f_m = mf_{rep} + \varepsilon \tag{5}$$

where f_{rep} is the repetition frequency, m is a large integer, and ε is the absolute frequency comb offset. For our purpose, however, we note that the pulse shaper acts as a frequency filter (schematically shown in red solid), whose center frequency provides a frequency reference, which we denote as f_s (red dash). To optimally select two comb lines via pulse shaping, the comb frequencies $\{f_m, f_{m+1}\}$ are aligned symmetrically about f_s by fine tuning the LCM position. This means that line frequencies referenced to f_s are:

$$\tilde{f}_m = (m - \frac{1}{2}) f_{rep} \tag{6}$$

regardless of the actual offset frequency ε. Figure 3(b) shows the two lines (blue dash) with the filter function magnified and plotted against $\tilde{f} \equiv f\text{-}f_s$. After alignment, if the comb offset varies from its initial value to $\varepsilon' = \varepsilon + \delta\varepsilon$ (green solid), what is observed by the pulse shaper is only the frequency offset change δε. Nonzero values of δε will eventually induce power loss as the lines approach the edges of the filter function, and this will transform into waveform variations in the time-domain. It is important to emphasize that only the relative frequency offset is important in line-by-line pulse shaping, not the absolute offset.

In Fig. 3(c) we show M(x) defined as a four-pixel passband filter (blue solid); 4 pixels are turned on with constant phase across the aperture. Recall that 4 pixels in our setup correspond to 2 comb lines. The effect of convolving a finite Gaussian beam (green dash) with a rectangular-like mask function will smear out the abrupt amplitude transitions at the pixel edges resulting in a non-rectangular $|H(\omega)|$, as shown in Fig. 3(d). Filter functions on a logarithmic vertical scale obtained experimentally by sweeping the wavelength of a CW laser (blue solid) and by simulation (green dash) are shown for comparison. The two selected spectral lines are indicated by red arrows.

#76023 - $15.00 USD Received 13 October 2006; accepted 10 December 2006

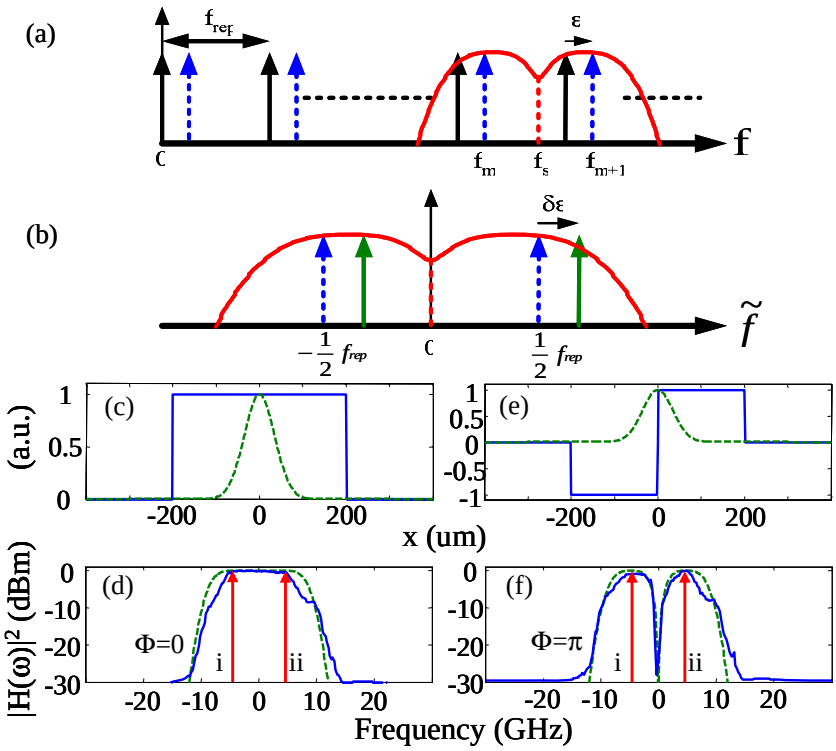

Fig. 3. (a). Optical comb in absolute frequency position (black solid arrows) and having an offset ε (blue dashed arrows). The schematic filter function is shown in red. (b) Two spectral lines selected by the pulse shaper are plotted against relative frequency after aligning the LCM (no additional offset: blue dash; with additional offset of δε: green solid). Mask function (solid line) and Gaussian intensity profile with radius w_0=75um (dashed line) for Φ=0 (c) for both lines and for Φ=π (e) to one line. Resulting 4-pixel passband filter function $|H(\omega)|^2$: (d) experimental (solid line) result by sweeping the wavelength of a CW laser and simulated (dashed line) for Φ=0; (f) experimental (solid line) and simulated (dashed line) for Φ=π. The arrows schematically indicate the comb line positions.

In Fig. 3(e), the lower frequency line (two left pixels) has an applied π phase shift, resulting in a negative mask field. Figure 3(f) shows the resulting experimental (blue solid) and simulated (green dash) |H(ω)| spectra in log scale - both reveal an obvious spectral dip. This dip can be understood as the field interference due to an abrupt spatial (π-0) phase transition; this results in diffraction of energy out of the main beam, which is eventually eliminated while coupling back into a single-mode optical fiber at the output of the pulse shaper.

In Fig. 3(f), the applied phase control induces a frequency-dependent transmission dip at the center of the passband. This dip functions as a frequency discriminator that is not present in the four-pixel passband filter with constant phase. This is the essential point used to explain the observed time-domain waveform instability shown in Fig. 2(d) when spectral phase control is applied. Under line-by-line phase control, H(ω) is no longer flat in the frequency-domain; thus a relative frequency offset ε_r in the optical comb will effectively be transferred to an extra energy loss by the central frequency discriminator. This loss viewed in the frequency-domain will result in large peak intensity variation in the time domain.

2.2 Data fitting and discussions

In Fig. 4(a) fit is shown to the experimental data presented in Fig. 2 using the frequency-domain model presented above. Figures 4(a) and 4(c) show the normalized optical spectral

#76023 - $15.00 USD Received 13 October 2006; accepted 10 December 2006

line amplitudes in linear scale with experimental frequency offset values. The 4-pixel bandwidth filter functions are included (shown in red dash) for Φ=0 (a) and Φ=π (c) applied to line {1}. Relative line amplitudes of the 0, 1, 2 and 3 lines are determined from the spectrum shown in Fig. 1(b). The necessity of using 4 comb lines is to reflect the fact that although only lines {1, 2} are selected at zero offset, additional lines from either side of the comb may participate in shaping for a large frequency offset (lines {0 or 3}, depending on the direction of frequency offset). Arrows indicate the initial line positions and the direction of increasing frequency offsets. Figures 4(b) and 4(d) show time-domain intensity waveforms corresponding to the various frequency offsets for Φ=0 (b) and Φ=π (d). The arrows indicate the evolution of amplitudes according to the change in frequency offset. The temporal delays of the waveforms (τ) as a result of the phase manipulation are also shown (dashed lines).

Comparing theoretical calculations shown in Fig. 4 and experimental results shown in Fig. 2 demonstrate excellent agreement. Several key features for discussion are: (i) For the Φ=0 case [Fig. 2(a) and Fig. 4(a)], only the amplitude of line {1} is attenuated. The amplitude of line {2} is not attenuated due to a change in frequency offset since the filter function is flat. The corresponding time-domain intensities [Fig. 2(b) and Fig. 4(b)] are therefore relatively insensitive to frequency offsets. Less than 35% variation in peak intensity occurs even for a 49% frequency offset. (ii) For the Φ=π case (Fig. 2(c) and Fig. 4(c), τ(π)=T/2), the amplitudes of both lines {1 and 2} are attenuated monotonically due to the increasing frequency offsets, due to the central transmission dip. The corresponding time-domain intensities [Fig. 2(d) and Fig. 4(d)] are therefore much more sensitive to change in frequency offset. For a 49% frequency offset, the change in I(τ(Φ)) is in excess of 95%. These two examples demonstrate the utility of the frequency-domain model, and provide a link with the time-domain picture provided in Ref. [4]. In particular, the time-domain picture predicts maximum intensity variation happens at odd multiples of T/2 (the temporal position centered between the original pulses), where contributions from adjacent pulses overlap and interact most strongly. With a phase step of Φ=π between adjacent spectral lines, the peak intensities are delayed to exactly odd multiples of T/2, therefore producing a large intensity variation.

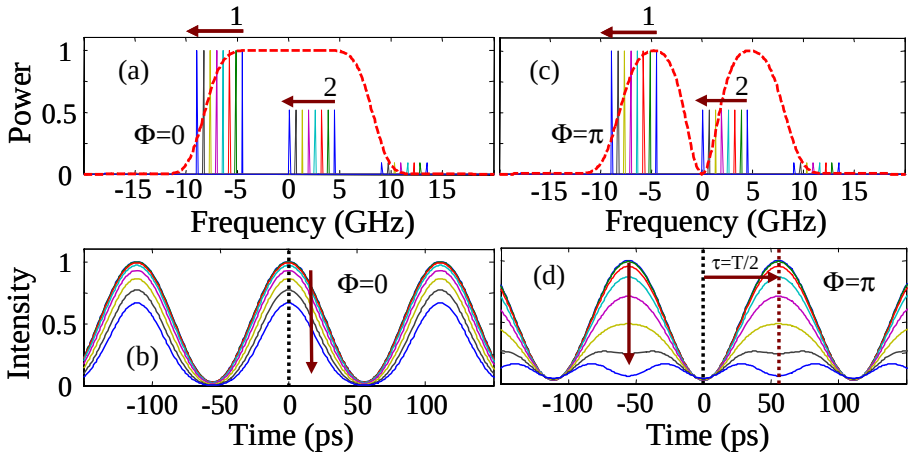

Fig. 4. Fit to Fig. 2 using the frequency-domain model. (a, c) Spectra fit (linear scale) for δε of {0, 7, 14, 21, 28, 35, 42 and 49}%. The arrows indicate the initial line positions and the direction of detuning. Experimental time-domain traces for corresponding frequency offsets are shown for Φ=0 (b) and Φ=π (d). The arrows indicate intensity peak variations associated with these frequency offsets. Delay positions are marked by dashed lines. (Video file of 0.97 Mb for Φ=0 and 1.00 Mb for Φ=π.)

Examination of the Φ=π amplitude variation [Fig. 2(d) and Fig 4(d)] shows that the periodicity of the waveforms gradually evolves to T/2 as the frequency offset increases. The

#76023 - $15.00 USD Received 13 October 2006; accepted 10 December 2006

origin of this repetition rate doubling is explored in Fig. 5. In Fig. 5(a), comb lines (arrows) and the filter function (red dash) are schematically sketched against relative frequency. The blue solid arrows show the initial comb line positions and the green dashed arrows show the comb with a frequency offset δε, while keeping line amplitudes fixed. The lines are spaced apart by f_{rep}. When one of the spectral lines has an applied π phase shift relative to the other line, the field of the filtered comb is depicted in Fig. 5(b), with one line having negative amplitude. The corresponding time-domain intensity is shown as the blue solid trace in Fig. 5(d), a cosine function having period of T with delay τ(Φ)=T/2. Figure 5(c) shows the resulting filtered comb with offset δε, constituting three lines denoted as {i, ii, iii}. Note that the amplitudes of all the lines are affected by the frequency-dependent transmission of the filter, while the signs read {+,+,-}, respectively. The corresponding time-domain intensity for the lines with this particular phase sequence, shown as the green dashed trace in Fig. 5(d), yields a shifted cosine function now with periodicity of T/2. This phenomenon can be understood from the beating between each two lines: the 9 GHz beating of lines {i, ii} almost cancels with that from {ii, iii}; what is left is the remaining 18 GHz beating between lines {i, iii}. The ability to predict subtle details of the experiment, such as the evolution of the intensity periodicity from T to T/2, again demonstrates the power of our frequency-domain treatment.

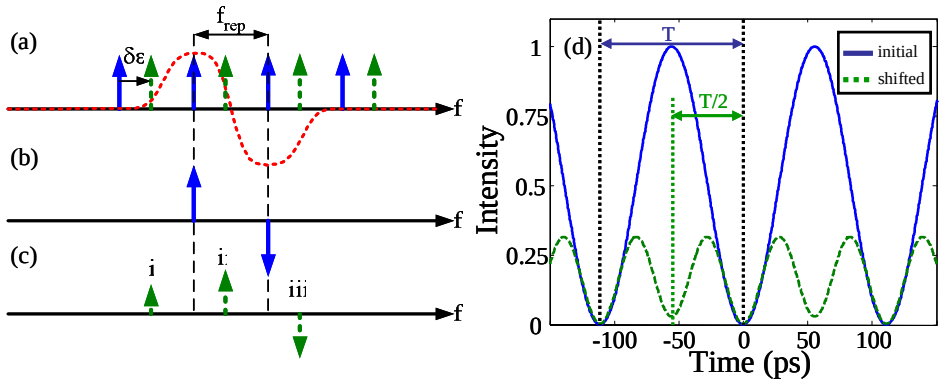

Fig. 5. Schematic of the concept of periodicity conversion due to shifting of the optical frequency comb when a phase shift is applied to one comb line. (a) Initial and the shifted frequency comb with fixed line amplitudes depicted by 4 arrows (solid: initial; dashed: shifted). The filter function is shown in red dashed line. (b) Filtered comb without frequency shift. (c) Filtered comb with a large frequency shift. (d) Simulated time-domain results showing periodicity conversion: from initial comb without frequency shift (solid) and the shifted comb (dash).

2.3 Correlating frequency and time-domain pictures: intermediate phases

Thus far phase steps between adjacent optical frequency comb lines have been limited to Φ=0 and π. This means the intensity waveform is shifted from 0 (temporal position with least impact to comb offset) to T/2 (position which is most vulnerable to offset) according to temporal delay τ(Φ) defined in Eqn. (1). In this section we examine other phase steps in order to investigate the dependence of the maximum peak amplitude variation on both frequency offset and delay.

Experimental and calculation results together with Φ=0 and π cases demonstrated previously are shown in Fig. 6. Figure 6(a) shows experimental (symbols), and calculated (lines), intensity values I(τ(Φ)) at δε of {0, 7, 14, 21, 28, 35, 42 and 49}%. Phase controls Φ are applied between 0 and π in π/4 increments to line {1}. The magnitudes of intensity variation increase with increasing τ(Φ) (in the direction of the black vertical arrow). Figure

#76023 - $15.00 USD Received 13 October 2006; accepted 10 December 2006

6(b) shows I(τ(Φ)) at δε=49% for different Φ values using a PMCW comb (blue circle: experimental; blue solid line: calculation). τ(Φ) is also included within the figure: experimental (diamonds) and calculation (dotted line). The perfect linearity of the trace indicates excellent control over phase settings to individual lines. In all calculations, the optical comb line amplitudes follow the experimental spectrum as shown in Fig. 1(b). Results show errors of less than 10% between experimental data and calculations. Together, Fig. 6(a) and 6(b) indicates that the amplitude change of I(τ(Φ)) increases monotonically both with frequency offset and temporal delay, in agreement with the time-domain view presented previously.

As a further example, calculated results of I(τ(Φ)) at δε=49% assuming an ideal comb comprised of equal amplitude lines (red square) are plotted against $\cos^2(\Phi/2)$ (red dashed line) in Fig. 6(b). Using the linear dependence of τ(Φ) on Φ, we infer that for an ideal comb, the range of intensity variation with frequency offset follows a temporal mask of the form $\cos^2(\pi f_{rep}\tau)$. We will use this empirical observation as an aid to interpret some of our later results.

Please note that the form of this relation may depend on pulse shaper resolution. In the current experiments, our pulse shaper spectral resolution is 1.7 times finer than the line spacing, which leads to a regime where the waveform interference in the time-domain is dominated by contributions from only nearest neighbor pulses. This corresponds most closely to the simple time-domain model put forth in Ref. [4].

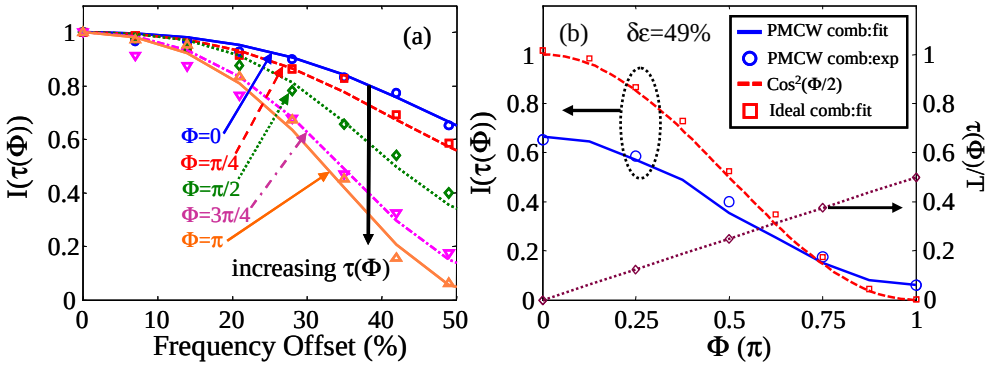

Fig. 6. (a). Experimental (symbols: Φ= {0, π/4, π/2, 3π/4 and π}) and calculated (lines: Φ= 0 to π in π/4 increments) waveform amplitudes at corresponding τ(Φ) for δε of {0, 7, 14, 21, 28, 35, 42 and 49}%. (b). Intensity values for 49% frequency offset at corresponding τ(Φ) for different Φ values using phase-modulated CW comb (blue circle: experimental; blue solid line: calculation). Calculated (dotted line) and experimental (diamonds) τ(Φ) is also included. Intensity values assuming ideal comb lines (red square) is plotted with $\cos^2(\Phi/2)$ (red dashed line).

3. Time-domain waveforms designed for monitoring optical frequency fluctuations

3.1 Design approach

As discussed above, phase manipulation of one spectral line for a two-line cosine time-domain waveform is sensitive to spectral frequency shifts. We can therefore ask the question: can line-by-line pulse shaping be used to monitor variations in the comb offset frequency, at least in the large fluctuation regime? For the purpose of frequency fluctuation monitoring, it would be useful to design waveforms that not only exhibit temporal positions that are sensitive to frequency fluctuation, but also have stable reference points. The existence of a reference point that is insensitive to optical frequency fluctuations would allow one to distinguish waveform changes arising from pure frequency fluctuations from the effects of laser intensity

#76023 - $15.00 USD Received 13 October 2006; accepted 10 December 2006

fluctuations. This should also increase the sensitivity of such a scheme for monitoring optical comb frequency fluctuations.

Based on the previous discussions, one simple choice of target waveform would be a time-domain cosine generated by selecting two spectral comb lines. In general, one can select any two spectral lines separated by Nf_{rep}, where N is an integer. For the N=1 example discussed above, we have shown that there is significant sensitivity to frequency fluctuations at time positions equal to odd multiples of T/2 but not at multiples of T. Let us assume that this behavior applies also for N>1, which is justified by the results given below. Then any two lines spaced apart by $2f_{rep}$ or greater will exhibit waveform positions both sensitive and insensitive to comb fluctuations, since there will be peaks situated at multiples of T/N. Furthermore, applying a phase shift onto one of the two lines allows us to finely shift the positions of the peaks for optimum sensitivity.

To illustrate this argument, Fig. 7 shows simulation results using the frequency-domain model. For simplicity, an ideal comb of f_{rep}=9 GHz spacing (T=111.1 ps) is assumed with spectral comb lines of equal amplitudes. Figure 7(a) shows a filter designed to select two lines spaced by $2f_{rep}$ (N=2) which removes the intermediate line. Optical frequency comb offsets of {0-50}% with 10% per step are indicated. The corresponding time-domain waveforms are shown in Fig. 7(b). I(0) is invariant while I(T/2) is sensitive to frequency fluctuations. The $\cos^2(\pi f_{rep}t)$ is plotted (green dashed line) to emphasize the temporal intensity variation relation discussed in the previous section. The ratio of I(T/2) to I(0) offers a clear indication of frequency offsets, especially for large offsets. Figure 7(c) shows the semi-log plot of the contrast ratio with various offset values. The scenario is different if one of the lines is π-shifted, shown in Fig. 7(d). Since the waveforms are delayed by T/4, all the peaks encounter the same amount of intensity variation. One interesting observation is how the $\cos^2(\pi f_{rep}t)$ function nicely cuts the intensity waveform at 50% offset. This once again supports our conclusion drawn from the previous section.

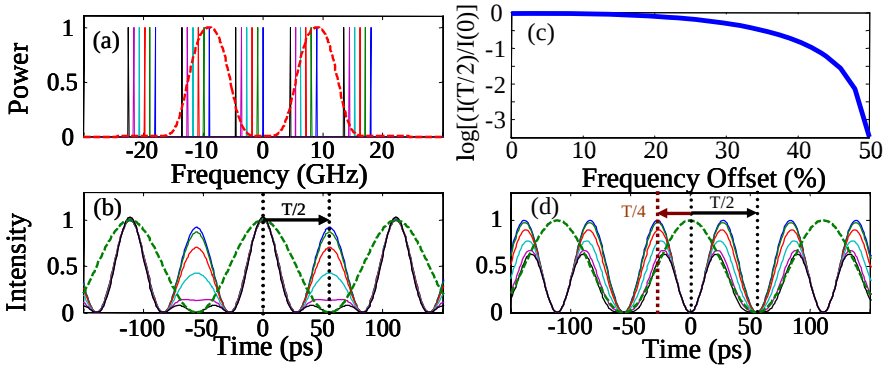

Fig. 7. Two lines selected at $2f_{rep}$ by blocking the center line. (a) Ideal comb lines shifted with δε {0-50}% in 10% increment with no phase control. (b) Resulting time-domain intensity: peak at time zero is stable while peak at time T/2 is sensitive to offsets. (c) Semi-log plot of I(T/2)/I(0). (d) Ideal comb lines shifted with offsets {0-50}% in 10% increment with Φ=π to one line. In (b, d), green dashed lines depict $\cos^2(\pi f_{rep}t)$.

3.2 Experimental results

A broader and flatter optical comb is favored for this experiment to better approach the ideal comb (equal intensities for the comb lines). A low V_π lithium niobate phase modulator (20GHz bandwidth, V_π of ~2.8V at 1 GHz) is modulated at f_{rep}=9GHz with a driving voltage of ~2.6 V_π peak to peak to obtain the spectrum shown in Fig. 8(a). Relative phases of the lines are measured for lines {-6 to 5}. Lines {1, 0, -3, and -5} are π out of phase with the rest, which agree with calculation using a Bessel series [8]. Figure 8(b) shows an expanded portion

#76023 - $15.00 USD Received 13 October 2006; accepted 10 December 2006

of the comb on a linear scale with line powers normalized to line {3}. Lines {2 and 4} are selected to pass through the pulse shaper while the others are blocked by applying amplitude control to the line-by-line shaper to obtain two spectral lines spaced by $2f_{rep}$.

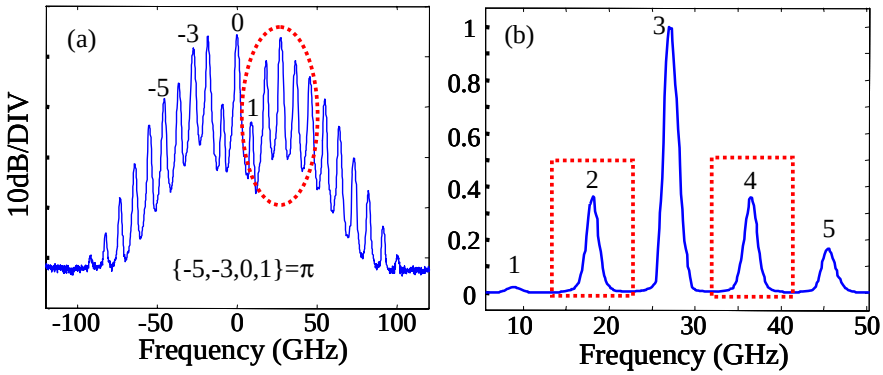

Fig. 8. (a). Spectrum obtained from a low V_π phase modulator. Circled spectral portion is expanded in (b), in linear scale and normalized to line {3}. Lines {2, 4} are selected by the line-by-line shaper while the others are suppressed.

Figure 9 shows experimental and calculated results for this waveform. Figures 9(a) and 9(b) show the experimental spectra and line amplitudes used in the calculation with $\delta\varepsilon$ of {0, 7, 14, 21, 28, 35, 42, and 49}%, both in linear scale. In both figures, the horizontal arrows indicate the initial line positions and the direction of detuning. In Fig. 9(b), the amplitudes of the spectral lines reflect the experimental spectrum shown in Fig. 8(b). Figures 9(c)-9(e) show resulting time-domain profiles for the various shifts of the frequency comb with phase Φ={0, π/2, and π} applied to line {2}, respectively. Figures 9(f)-9(h) show the corresponding calculated intensities reflecting the experimental conditions. In Figs. 9(c)-9(h), vertical arrows indicate intensity variations as the optical frequency offset increases for different temporal positions; zero delay and T/2 positions are marked as an aid to the eye.

Again the agreement between data and theory is excellent. Even the detailed features observed at large frequency offsets show excellent correspondence. For example, both Figs. 9(c) and 9(f) show the repetition period changing from T to T/2; both Fig. 9(d) and 9(g) show temporal shifts in the peak near T/2; and both Figs. 9(e) and 9(h) show symmetric waveform shifts about t=0. In the end, it is the waveform with Φ=0 (c and f) that is of primary interest for monitoring of optical comb frequency shifts. In contrast to Fig. 7(b), where intensity values at I(0) are invariant to frequency offsets, I(0) in Figs. 9(c)-9(f) increases slightly with increasing frequency offset. This results in an enhanced sensitivity to frequency shifts and is attributed to the unevenness of the PMCW line powers in Fig. 8(b). Under large frequency offset, the strong central line {3} that is initially blocked contributes to pulse shaping and accelerates the variation in the intensity waveforms.

#76023 - $15.00 USD Received 13 October 2006; accepted 10 December 2006

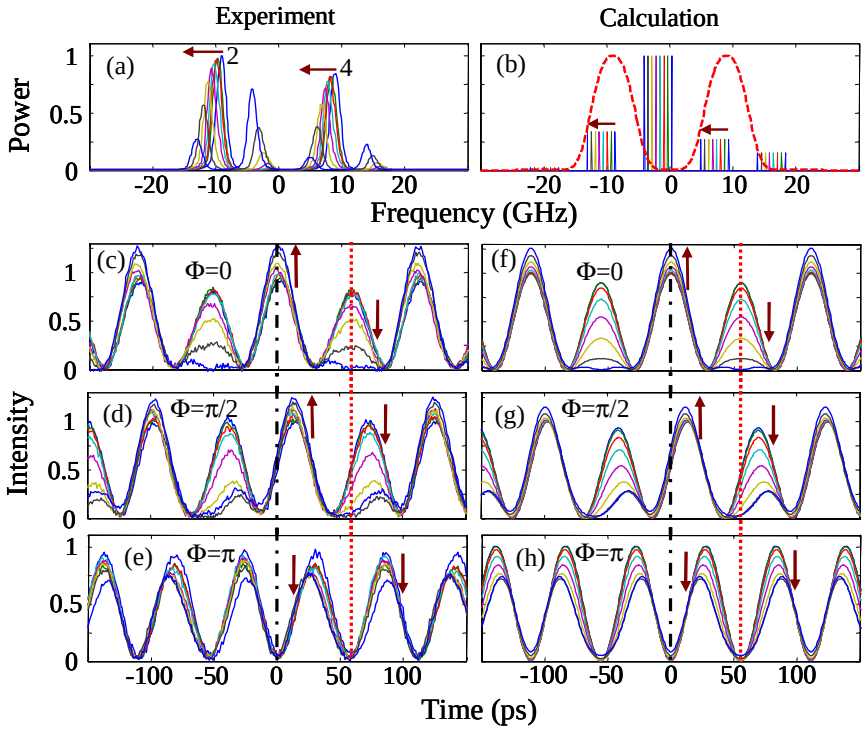

Figs. 9. (a). and (b). Experimental spectra and the lines used for calculation (linear scale) for two lines with spacing of $2f_{rep}$ with $\delta\varepsilon$ of {0, 7, 14, 21, 28, 35, 42, and 49}%. The horizontal arrows indicate the initial line positions and the direction of detuning. (c-e) Experimental time-domain waveforms for Φ={0, π/2, and π}, respectively. (f-h) Calculated time-domain waveforms for Φ={0, π/2, and π}, respectively. The vertical arrows indicate intensity variations as the optical frequency offset increases for different temporal positions. Temporal positions: dash-dot: zero delay; dashed: T/2.

3.3 Larger N values

One may extend the spacing between the two selected lines to achieve similar results. Figure 10 shows simulation results for an ideal (equal amplitude) comb for N=3 (a-d) and N=4 (e-h). Note how well the frequency-offset intensities correspond to the $\cos^2(\pi f_{rep}t)$ function. The time-domain picture is clearly illustrated: frequency sensitivity of waveforms generated via line-by-line pulse shaping in the 100% duty cycle regime is least noticeable at time positions equal to 0 (or integral multiple of the repetition period T) and increasingly noticeable for increasing time offsets. Maximum intensity variations with frequency offsets occur for time positions of T/2 and its odd multiples.

#76023 - $15.00 USD Received 13 October 2006; accepted 10 December 2006

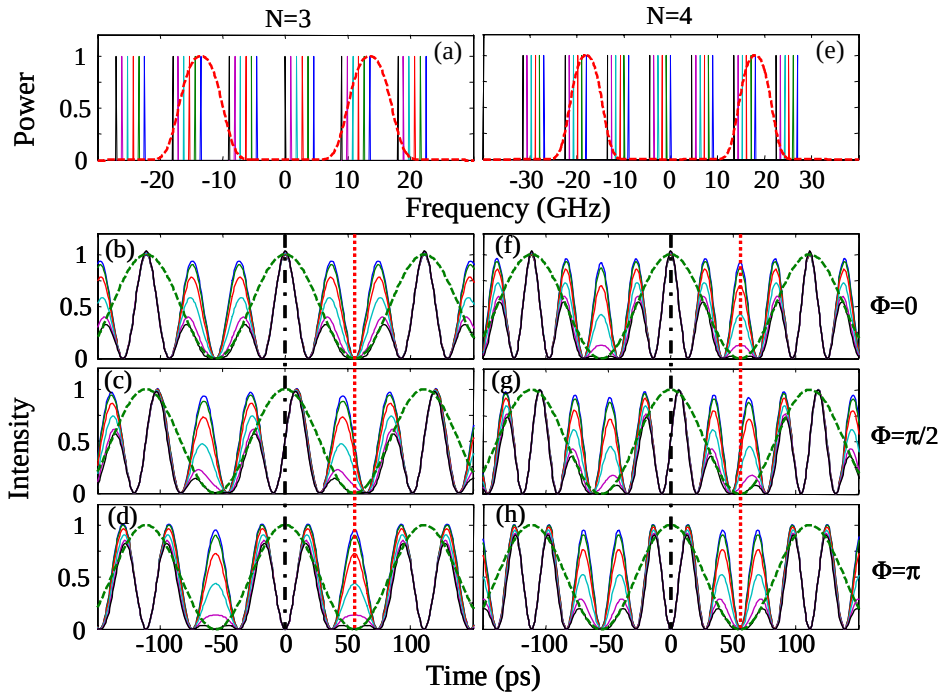

Fig. 10. Simulation spectra for two lines with N=3 (a) and N=4 (e) with δε of {0-50}% in 10% increments. Resulting time-domain waveforms are given for N=3 (b-d) and N=4 (f-h) with phase shifts applied to one line Φ={0, π/2, π}, respectively. Green dashed lines depict $\cos^2(\pi f_{rep} t)$. Temporal positions: dash-dot: zero delay; dashed: T/2.

4. Conclusion

In summary, the impact of frequency comb shifts on time-domain waveforms generated through line-by-line shaping has been quantitatively investigated. The influence of frequency offset on generated waveforms is explained from both time and frequency-domain perspectives. A quantitative frequency-domain model is provided starting from pulse shaper theory. Time-domain intensity variations that have previously been observed in pulse shaping due to an unstable mode-locked frequency comb are experimentally emulated using a wavelength detuned phase-modulated CW laser, which allows quantitative analysis. The experimental data are in excellent agreement with the predictions of our frequency-domain model. Finally, we propose and model pulse shaper waveforms that should be useful for monitoring the optical frequency fluctuations of the input comb.

Acknowledgments

This work is supported by Air Force Office of Scientific Research/DARPA grant FA9550-06-1-0189.

#76023 - $15.00 USD Received 13 October 2006; accepted 10 December 2006